abdA expression in *Drosophila* embryos

François Karch,[1] Welcome Bender,[2] and Barbara Weiffenbach[2]

[1]Department of Animal Biology, University of Geneva, 1224 Geneva, Switzerland; [2]Department of Biological Chemistry and Molecular Pharmacology, Harvard Medical School, Boston, Massachusetts 02115, USA

The *abdominal A* (*abdA*) gene is one of three transcription units in the Bithorax Complex of *Drosophila* encoding a homeo box protein; it is flanked by *Ultrabithorax* (*Ubx*) and *Abdominal B* (*AbdB*). The *abdA* gene is required for segmental identity of the second through eighth abdominal segments. The transcription unit of *abdA* is ~20 kb long and encodes a protein of 330 amino acids. The *abdA* homeo box is almost identical to the homeo box of *Ubx* but is quite different from the *AbdB* homeo box. A polyclonal antibody to *abdA* protein stains embryonic nuclei in segments A1–A7 (parasegments 7–13). The *iab-2, 3,* and *4* mutant classes define positive *cis*-regulatory elements that induce expression of *abdA* in segments A2–A4 (parasegments 7–9), respectively. Once a pattern of *abdA* expression is turned on in a given parasegment, it remains on in the more posterior parasegments, so that the complex pattern of expression is built up in the successive parasegments. The *abdA* product appears to repress expression of *Ubx* whenever they appear in the same cell, but *abdA* is repressed by *AbdB* only in the eighth and ninth abdominal segments.

[*Key Words*: *abdA*; *Drosophila*; *Ubx*; homeo box; Bithorax Complex]

Received March 20, 1990; revised version accepted June 14, 1990.

The Bithorax Complex (BX-C) is responsible for segmental identity of the third thoracic segment (T3) and eight abdominal segments (A1–A8). Lewis (1978) showed that in embryos lacking the BX-C, all of these segments develop like copies of T2. A large number of nonlethal mutations in the complex have been isolated (for review, see Duncan 1987). The majority of alleles have their most dramatic effects on a single segment-wide band of the insect body. The affected bands correspond to parasegments (Martinez-Arias and Lawrence 1985); each parasegment includes the posterior compartment of one segment and the anterior compartment of the next segment. The recessive loss-of-function mutations typically transform a particular parasegment into a copy of the anterior adjacent parasegment. These mutations have been grouped in nine classes called *abx/bx*, *bxd/pbx*, *iab-2*, *iab-3*, *iab-4*, *iab-5*, *iab-6*, *iab-7*, and *iab-8,9*. These mutant classes affect primarily parasegments 5–13, respectively.

There are three additional classes of loss-of-function mutations that cause more extensive transformations and usually result in embryonic or larval lethality. These classes are designated *Ultrabithorax* (*Ubx*), *abdominal A* (*abdA*), and *Abdominal B* (*AbdB*) (Sanchez-Herrero et al. 1985; Tiong et al. 1985). An apparent *Ubx abdA AbdB* triple mutant chromosome causes embryonic transformations equivalent to those of a deletion for the entire complex, and so, it has been proposed that these mutations mark three products that account for most or all of the functions of the complex (Casanova et al. 1987). The parasegment-specific viable mutations might therefore affect *cis*-regulatory regions for the three major products. Complementation patterns support this view. All *abx/bx* and *bxd/pbx* mutations fail to complement with strong *Ubx* alleles, and so, these might be regulatory regions for the control of expression of the *Ubx* product. Likewise, the *iab-2*, *iab-3*, and *iab-4* mutations might mark regulatory regions for the abdA product, and the *iab-5*, *iab-6*, *iab-7*, and *iab-8,9* mutations might affect the expression of the *AbdB* product (Karch et al. 1985; Sanchez-Herrero et al. 1985; Tiong et al. 1985).

The BX-C has been cloned and covers 300 kb of DNA (Bender et al. 1983; Karch et al. 1985). Because the presumed regulatory mutations are virtually all due to chromosomal rearrangement breaks, to deletions, or to insertions of transposons, it has been possible to localize >100 mutant lesions on the DNA map. They are spread over the entire complex, and they lie on the chromosome in the same order as the body segments they affect (Lewis 1978; Bender et al. 1983; Karch et al. 1985; Duncan 1987). DNA lesions associated with *Ubx*, *abdA*, and *AbdB* mutations are localized in the midst of their respective regulatory regions, and for *Ubx* and *AbdB*, the lesions disrupt large transcription units encoding their respective products. For *Ubx*, there are multiple products derived by alternate splicing, but all mRNAs include a 3′ exon encoding a homeo box protein sequence (Beachy et al. 1985; O'Connor et al. 1988, Kornfeld et al. 1989). The homeo box domain is a DNA-binding region, as inferred initially from homology to bacterial and yeast DNA-binding proteins (Laughon and Scott 1984; Gehring 1987). The *AbdB* transcription unit makes multiple RNA products by both alternate promoters and alternate splicing, but again all products include a pair of exons encoding a homeo box domain

(Celniker and Lewis 1987; Celniker et al. 1989; DeLorenzi et al. 1988; Kuziora and McGinnis 1988; Zavortink and Sakonju 1989). This report describes the analogous transcription unit and protein product for *abdA*.

Initially, it was difficult to imagine how only three families of protein products could account for the phenotypic diversity of all of the mutations of the complex. However, antibodies to the *Ubx* protein products reveal that the pattern of *Ubx* expression is very intricate. The *abx/bx* alleles affect parts of the pattern in PS5, and *bxd/pbx* mutations perturb the *Ubx* pattern in PS6 (White and Wilcox 1984, 1985; Beachy et al. 1985; White and Akam 1985). In our working model, *cis*-regulatory elements that program the patterns of the *Ubx*, *abdA*, and *AbdB* proteins are arranged along the chromosome in parasegment-specific groups (Peifer et al. 1987). Here, we present new evidence for the model from the *abdA* domain.

Results

The *abdA* region of the BX-C is shown in Figure 1. Two new chromosomal rearrangement breaks from E.B. Lewis have been localized in this region at positions +32.5 kb (*iab-2*^{671}) and +55.5 kb (*iab-3*^{33}). Flies hemizygous for these two mutations survive to adulthood and show segmental transformation of the *iab-2* and *iab-3* type, respectively (Karch et al. 1985). All of the available rearrangement breaks between *iab-2*^{671} and *iab-3*^{33} are embryonic lethal *abdA* mutations (Karch et al. 1985; Sanchez-Herrero et al. 1985; Tiong et al. 1985). This region of lethal breakpoints coincides with the abdA transcription unit (see below).

The abdA transcription unit and protein

The *abdA*^{C26} mutation is a 1.4 kb deletion that removes the M repeat sequence lying at +35 kb (Karch et al. 1985; Regulski et al. 1985). The lesion had been cloned, and we used a 1.2 kb *Bam*HI–*Sal*I fragment carrying the deletion to screen an embryonic cDNA library of M. Goldschmidt-Clermont. A few clones were isolated, of which 1dB-5 had the largest insert of 1.8 kb. When used as a probe on a genomic blot of the *abdA* region, 1dB-5 hybridizes to restriction fragments around +35 and +55 kb. These two regions are affected by two *abdA* deletions (*abd-A*^{C26} and *abd-A*^{MX2}). The complete sequence of 1dB-5 is shown in Figure 2, and its features are diagrammed in Figure 1. We also sequenced the genomic fragments that encode the exons and confirmed the exon sequences with other cDNAs. The deduced splicing map of the *abdA* transcription unit is shown below the genomic map of Figure 1. The sequence includes 7 exons (numbered 2 through 8). The gene is transcribed from right to left relative to the genetic map (in the same direction as *Ubx* and *AbdB*), as determined by the orientation of the homeo box-coding sequence and by Northern analysis with strand-specific probes (data not shown). The exon/intron boundaries (Fig. 2) are in nearly perfect

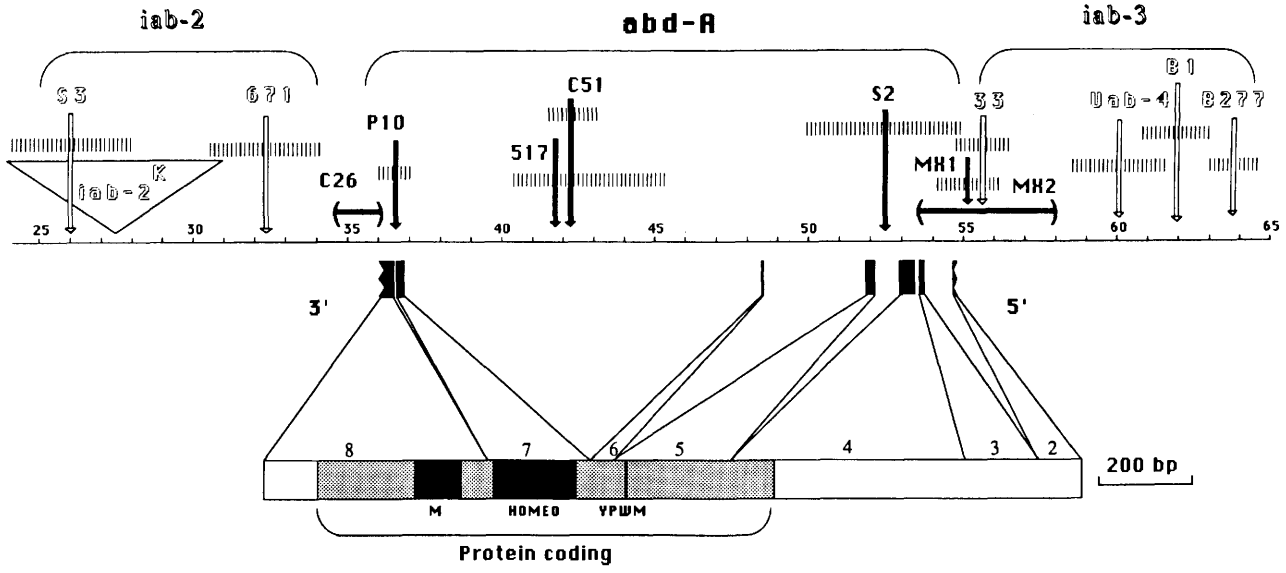

Figure 1. The *abdA* transcription unit. The thin horizontal line in the middle of the diagram represents the genomic DNA of the *iab-2*, *abdA*, and *iab-3* regions, marked off in kilobases. The *iab-2* and *iab-3* mutations are viable and affect PS7 and PS8, respectively. They are shown outlined on top of the genomic DNA by vertical arrows, indicating chromosomal rearrangement breaks, and by a large triangle representing a gypsy transposon. The lethal *abdA* mutations are represented in black. Thick horizontal lines indicate deletions. The seven exons found in the 1dB-5 cDNA are represented below the genomic DNA. Jagged edges at the 3′ and 5′ ends indicate that the cDNA is not full length at either end. A more 5′ exon is found in other *abdA* cDNA clones, and so, the first exon of 1dB-5 is labeled 2. Note that the genomic region coding for 1dB-5 coincides with the DNA domain defined by *abdA* mutations. Features of the 1dB-5 sequence are summarized at the *bottom* of the figure at a different scale. The sequence is represented by a rectangular box with the *abdA* open reading frame shaded. The M repeat, homeo box, and YPWM conserved motifs are shown.

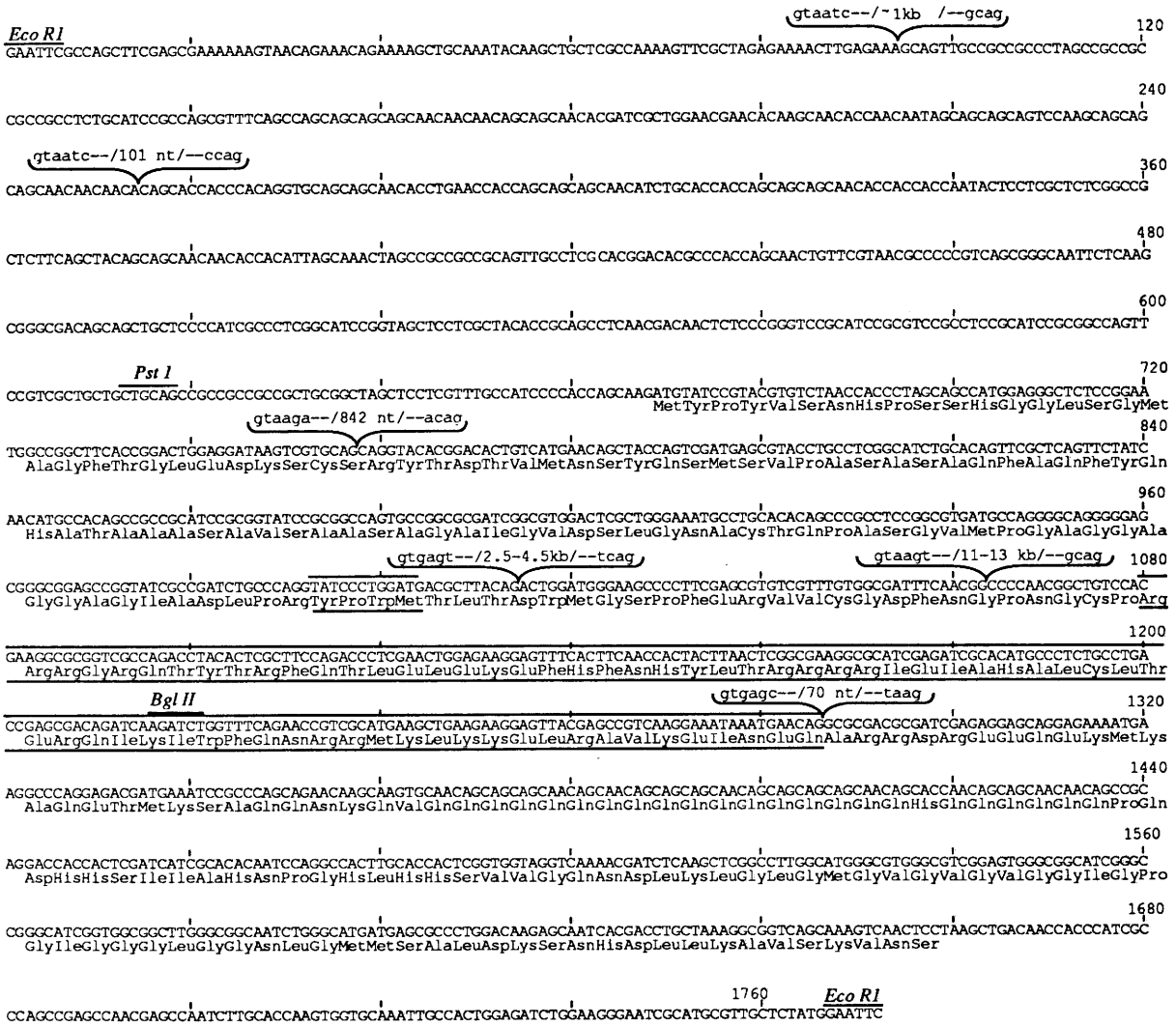

Figure 2. DNA sequence of the 1dB-5 cDNA. The DNA sequence of the noncoding strand of 1dB-5 is shown in the 5′ to 3′ orientation. Several restriction sites are shown on top of the sequence, as well as the sites of the six introns that interupt the sequence. Although the *Eco*RI site at the 3′ end was added during the construction of the cDNA library, the 5′ *Eco*RI site is encoded by the genomic DNA. The sequences of the third, fourth, and seventh introns were determined but are not shown. The amino acid sequence of the *abdA* protein encoded by 1dB-5 is shown below the DNA sequence. The YPWM motif and homeo box are flanked by bars.

agreement with the proposed consensus sequence (Breathnach and Chambon 1981; Mount 1982). We used a subclone from the 5′ end of the 1dB-5 cDNA as probe on a Northern blot, and we detected two transcripts of 5.1 and 5.4 kb in 2- to 4-hr embryos, which remain present through the rest of development (data not shown; Rowe and Akam 1988). Thus, 1dB-5 is only a partial cDNA, and we are currently analyzing additional cDNAs. Preliminary mapping of other cDNA clones indicates that most of the size difference lies in the 3′-untranslated region, but there is an additional short exon at the 5′ end (numbered 1) transcribed from +55.6 on the map (H. Jijakli and F. Karch, in prep.). Because the next chromosomal rearrangement break (*iab-3*[33], Fig. 1) is viable and shows segmental transformation of the *iab-3* type, the *abdA* promoter must lie between +55.6 and +57. In the 1dB-5 sequence, a short rearrangement occurred near the 3′ end, so that the last 67 bases of the sequence shown in Figure 2 are inverted relative to the genomic DNA.

The longest open reading frame in 1dB-5 is 1545 nucleotides long (from 114 to 1659; see Fig. 2) and contains the *abdA* homeo box, but the first ATG triplet is found at position 669, and so, the largest putative protein encoded by 1dB-5 is 330 amino acids long. This protein corresponds to an *abdA* product, as shown by immunostaining of whole embryos (see below). It is unlikely that the reading frame upstream of the ATG is translated, as an antibody raised against a segment of this upstream open reading frame (from nucleotide 255 to 618) fails to stain developing embryos.

The homeo box homology is found from nucleotides 1080 to 1259 (see Fig. 2). The homology with *Ubx* extends 9 amino acids beyond the carboxyl end of the 60-

amino-acid homeo box, up to the position of a 70-bp intron in the *abdA* transcript (Fig. 2). The *abdA* transcript is unlike *Ubx* or *Antp* in that the homeo box exon is separated from the 3′-coding region by this short intron. Another sequence in common with the *Ubx*, *Antp*, and *Dfd* proteins is the peptide Tyr-Pro-Trp-Met (YPWM) found upstream from the homeo box at position 993 (see Fig. 2). An *opa* or M repeat sequence is found in the coding region downstream of the homeo box. This repeat is composed of $(CAA)_n$ or $(CAG)_n$, and it encodes a stretch of polyglutamine as it does in *Notch* (Wharton et al. 1985). 1dB-5 also contains a 48-nucleotide microexon sequence preceding the homeo-box exon. We are examining other cDNAs to learn whether they contain additional or alternative microexons, as was found for the *Ubx* transcription unit.

We have raised a polyclonal antibody directed against a segment of *abdA* to study the spatial distribution of the *abdA* protein. The *Pst–Bgl*II fragment from nucleotide 618 to nucleotide 1216 (see Materials and methods; Fig. 2) was cloned into the *Pst* and *Bam* sites downstream of the pEX-2 gene contained in the bacterial expression vector of Stanley and Luzio (1984). The resulting fusion peptide contains the amino-terminal half of the *abdA* protein, but it lacks the final third of the homeo box and the carboxy-terminal sequences, including the M repeat. The fusion protein also contains 17 amino acids encoded by the leader region upstream of the ATG at position 669 (Fig. 2). The fusion product was eluted from an SDS–polyacrylamide gel and injected into a rabbit. Harvested serum was first depleted against pEX bacterial extracts and then affinity-purified on a column coupled with the fusion protein (see Materials and methods).

abdA *protein pattern in wild type*

abdA antigen is detectable first in embryos at ~4 hr of development, when the extension of the germ band is almost complete (Fig. 3A). *Ubx* antigen appears at about the same time, although the earliest signal is very weak and the relative sensitivities of the two antisera are unknown. For both *abdA* and *Ubx*, the antigens appear more or less simultaneously in all expressing parasegments (Fig. 4A). By 5 hr, the staining becomes much more intense (Fig. 3B), although the pattern does not change; the staining seems confined to the nuclei. *abdA* protein appears in seven bands of nuclei across the epidermis and in nuclei of the amnioserosa. The most anterior band begins at the front edge of PS7, and all but the most posterior band are one parasegment wide. Each band is intense at the anterior border of the parasegment and grades uniformly to nearly no staining at the posterior border of the parasegment. The pattern is complementary to the *Ubx* pattern in PS7–PS12 (Fig. 4A), which is strong in the posterior but weak in the anterior of each parasegment. The *abdA* antigen in PS13 does not extend to the posterior edge of the parasegment (Fig. 3).

By the beginning of germ-band retraction (~7.5 hr), *abdA* appears beneath the epidermis in the mesodermal cells that flank the developing gut. Strongly staining cells surround the spiracle pits, and some of the neuroblasts near the midline also stain. After germ-band shortening (Fig. 3C), segmental grooves appear in the anterior part of each parasegment, and *abdA* protein appears strongly in epidermal nuclei on either side of the grooves in PS7–PS12 and more weakly in the epidermal nuclei in the middle of segments A2–A7. The protein is restricted to the anterior side of the groove separating segments A7 and A8. By this time, the anterior and posterior midgut rudiments have joined, and the visceral mesoderm is adhering to the gut. *abdA* protein appears in the nuclei of the visceral mesoderm in PS8–PS12. Mesoderm positions were determined relative to *ftz* expression stripes by staining embryos containing a *ftz–lacZ* fusion (Hiromi and Gehring 1985) simultaneously for *abdA* protein and β-galactosidase (Fig. 4F). The staining of nuclei in the developing tracheal tubes is also apparent by this stage.

By ~10 hr (Fig. 3D), a pattern of strongly staining nuclei appears in the ventral nerve cord in segments A2–A7. (When we are not sure whether the pattern boundaries are segmental or parasegmental, as in the nervous system, we describe the patterns in relation to the more obvious segments.) The epidermal and neural patterns look almost identical from A2 through A7, but the staining intensity increases in the more posterior segments. The two bands of visceral mesoderm staining begin to broaden and split. In late embryos and first-instar larvae, the stained cells of the visceral mesoderm form four lines of nuclei evenly spaced around the gut (Fig. 3F). The anterior limit of *abdA* staining in the visceral mesoderm meets the posterior limit of *Ubx* staining (Fig. 4E), which at 12 hr lies in the prominent anterior furrow of the gut sac. The posterior limit of *abdA* is just anterior to the branching point of the Malpighian tubules, at the junction of the midgut and hindgut. At ~10 hr, a line of strongly staining cells adheres to the visceral mesoderm along the entire midgut. These cells make tracheal tubes that branch from four larger dorsal–ventral tubes, which underlie the segmental boundaries from A1/A2 through A4/A5; these branches adhere to each other and run anteriorly along the sides of the gut beneath the thoracic segments. The tracheal anatomy is clear in a transformant strain that makes β-galactosidase in cells of the tracheal system (M. O'Connor, J. Simon, and W. Bender, unpubl.).

As the epidermis closes at the dorsal midline (~11 hr), two lines of strongly staining nuclei at the dorsal borders of the epidermis come together (Fig. 3F) and form the posterior part of the heart. In older embryos, *abdA* staining is clear in the pericardial cells surrounding the heart tube, beginning in posterior A5 and extending back through A6 and A7 (Fig. 3G). Strong staining also appears in nuclei of lateral muscle fibers attached to the heart; the stained muscles underlie the segmental boundaries from A4/A5 to A7/A8. The gonads, which form beneath the A5 epidermis, also stain weakly in late embryos. The staining is in the somatic cells but not in the large germ line cells (Fig. 3G).

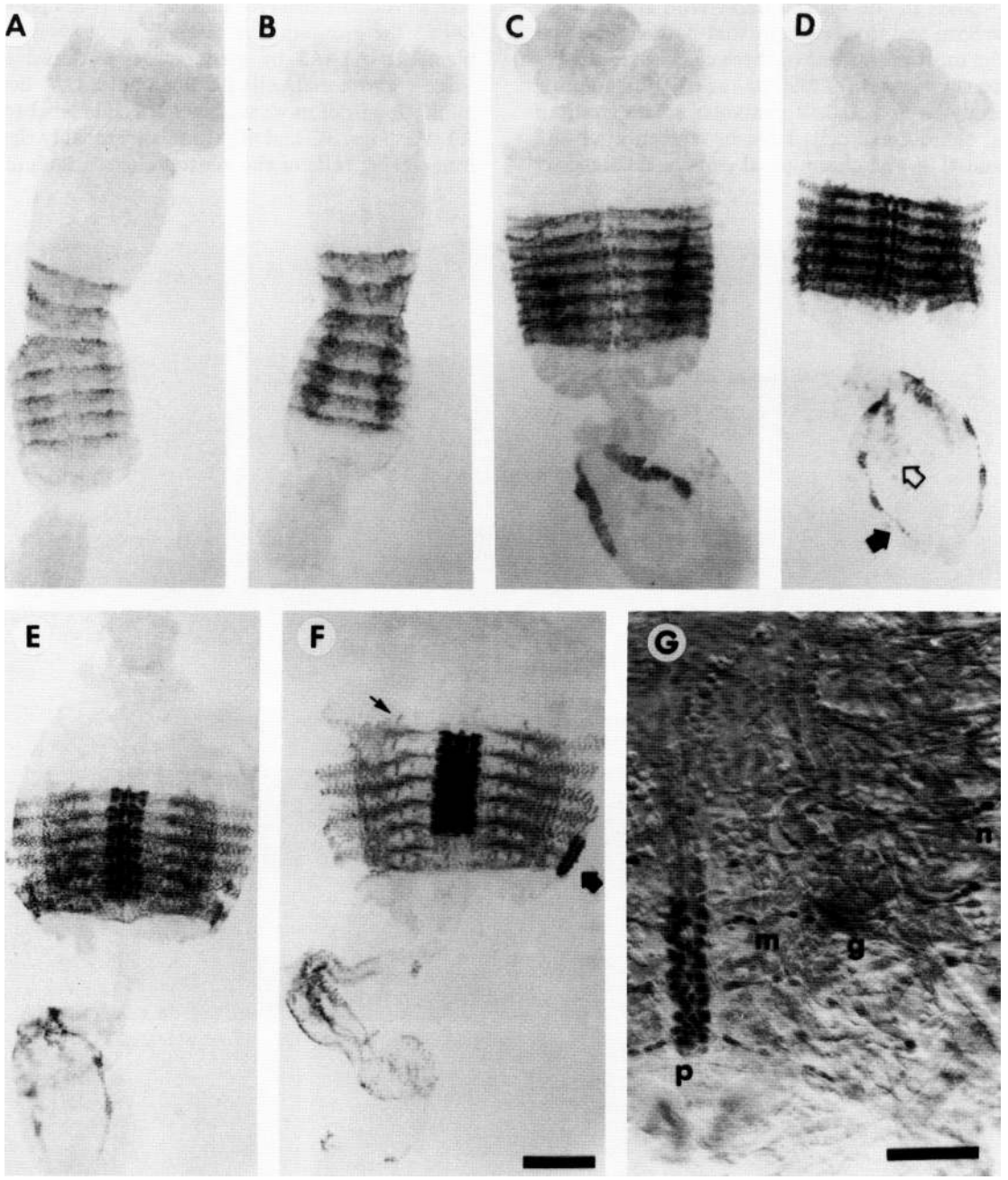

Figure 3. *abdA* protein pattern in wild-type embryos. Embryos were stained with a peroxidase-coupled secondary antibody, opened along the dorsal midline (*A–F*) or ventral midline (*G*) of the epidermis, and mounted with the gut folded out below the epidermal sheet. (*A*) About 4 hr, when *abdA* is first detected. The extended germ band was unfolded and flattened. (*B*) About 6 hr, mid-germ-band extension stage. (*C*) About 9 hr, after germ-band retraction. Staining is predominantly in the epidermis, especially at the segmental groves. *abdA* also appears in the visceral mesoderm. (*D*) About 10 hr, the *abdA* antigen appears in the neuroblasts along the midline. The open arrow shows the anterior limit of visceral mesoderm staining; the solid arrow points to the labeled tracheal cells along the gut. (*E*) About 12 hr, at the start of the nerve cord contraction. *abdA* staining decreases in the epidermis. (*F*) About 14 hr. The epidermis has closed at the dorsal midline. The thin arrow points to the line of nuclei of the chordotonal sense organs in the first abdominal segment. The thick arrow points to two lines of labeled cells that will form the posterior part of the heart. (*G*) Inner dorsal surface of a late embryo photographed with Nomarski optics. *abdA* antigen appears in the pericardial cells (p) and in the lateral muscle fibers (m) attached to the heart. Staining of the pericardial cells begins in posterior A5 and extends through A6 and A7; the stained muscle fibers underlie the four segmental boundaries from A4/A5 to A7/A8. In the gonad (g), the somatic cells surrounding the large germ line cells are weakly stained. A cell of the intersegmental nerve (n) stains strongly at the anterior edge of segments A4–A7. *A–F* are at equivalent magnification; bars, 100 μm (*F*); 50 μm (*G*).

The epidermal staining of *abdA* fades in late embryos, until it is undetectable in first-instar larvae. Strong staining persists in the ventral nerve cord and the visceral mesoderm and in a few cells that underlie the epidermis. The most prominent of these cells are in the peripheral nervous system (PNS), as revealed by staining with antibody to horseradish peroxidase. The group of five lateral chordotonal cells label in segments A1–A7 (Figs. 3F and 4G). The chordotonal cells in A1 lie anterior to the anterior margin of *abdA* staining in the epidermis, but they may still be derived from PS7 (posterior A1). In mutant embryos lacking the *abdA* gene (*DpP10; DfP9*), the group of five lateral chordotonal cells is replaced in A1–A7 by a thoracic-type dorsal cluster of three chordotonal cells (R. Bodmer and W. Bender, unpubl.). A pair of more ventral PNS cells label strongly in A2–A7 (Figs. 3G and 4I); these are probably the tracheal innervating cells of the ventral cluster (Bodmer and Jan

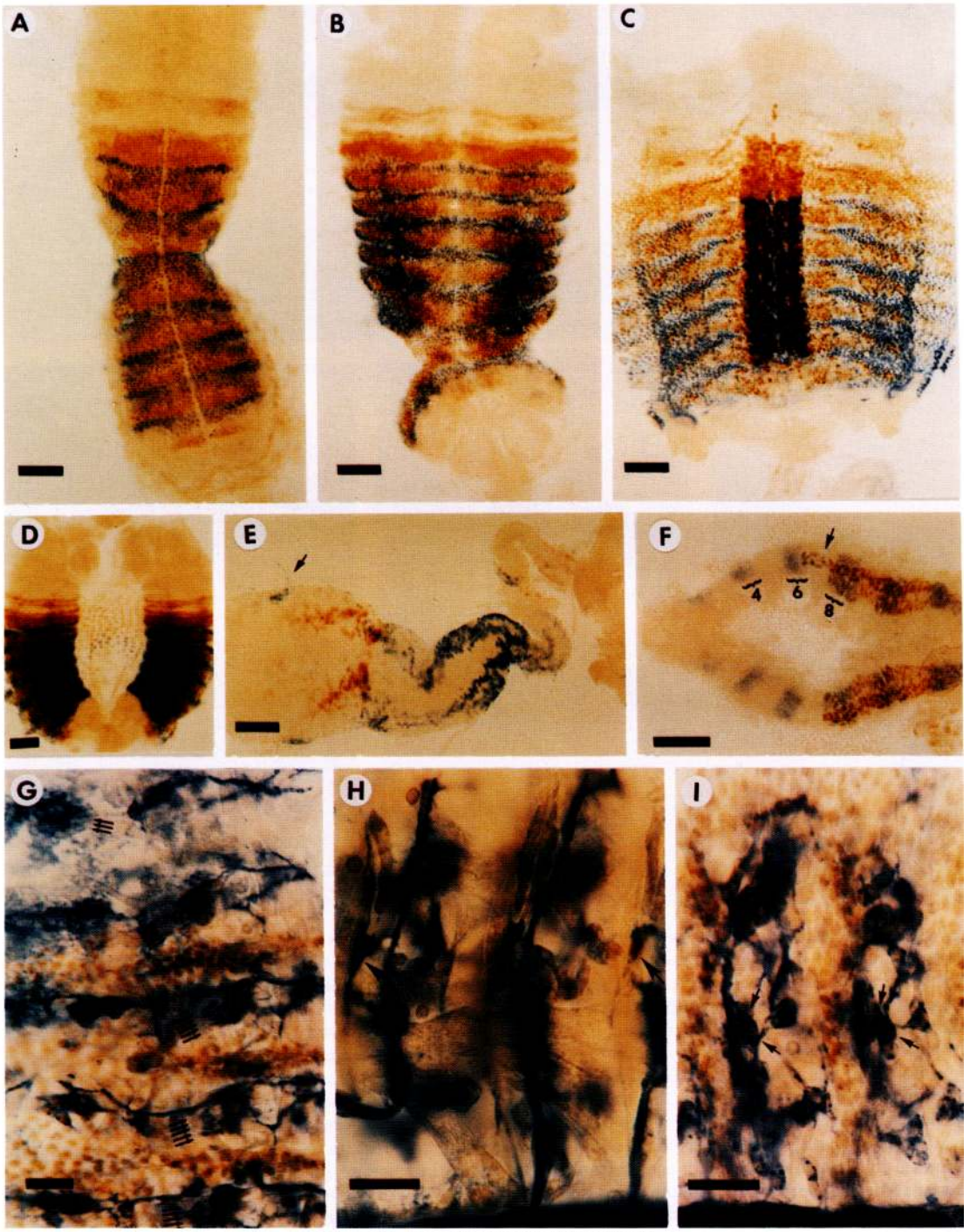

Figure 4. *(See facing page for legend.)*

1987). Finally, a single internal cell labels strongly beneath each segment border from A3/A4 through A6/A7 (Figs. 3G and 4H). This is the bipolar cell of the intersegmental nerve (Bodmer and Jan 1987); the tracheal innervating cell adjacent to each bipolar cell sometimes stains weakly.

We have not yet studied the patterns of *abdA* protein in stages beyond the first-instar larva.

Patterns in loss-of-function mutants

abdA *alleles* We stained *abdA* mutants as a control for the specificity of our antibody. Embryos homozygous for the $abdA^{MX1}$ rearrangement (Fig. 1) have no detectable staining, as expected, but we were surprised to see some antigen in many of the other alleles. Two alleles showed a near normal pattern of staining but with reduced intensity: $abdA^{C26}$, a small deletion (Fig. 1), and $abdA^{D24}$, an apparent point mutation (Karch et al. 1985). The $abdA^{C26}$ allele appears to have partial *abdA* function, as judged by embryonic transformations (Busturia et al. 1989). The $abdA^{MX2}$ deletion homozygotes show very weak staining in both the epidermis and nerve chord. The expression is too weak to compare it in detail to the wild-type pattern, but the nerve cord staining appears more graded than in wild type, with very weak expression in A2 and A3 and higher expression in A4–A7. Busturia et al. (1989) suggested that $abdA^{MX2}$ (and also $abdA^{MX1}$) might not be completely inactive. The *abdA* transcription start site described above maps within the $abdA^{MX2}$ deficiency, and so we presume another start site is used in $abdA^{MX2}$ homozygotes. We do not know whether such an alternate low-level start site could be used in wild-type embryos. The $abdA^{C51}$ and $abdA^{517}$ rearrangements (Fig. 1) have no detectable antigen except for weak staining in late embryos in the cells of the heart tube. The entire heart tube is stained in $abdA^{517}$ but the staining does not extend anterior to A5 in $abdA^{C51}$. These expression patterns could reflect position effects peculiar to these rearrangements.

Ubx *and* AbdB The *abdA* protein pattern was examined in embryos lacking the other proteins of the BX-C, to test for possible repression or enhancement in cells where two or more proteins are made. Embryos homozygous for the Ubx^1 mutation or deficient for the entire *Ubx* transcription unit ($Dfbxd^{100}$ homozgyotes) had wild-type *abdA* patterns. In embryos homozygous for the most extreme class of *AbdB* alleles (*D16* or *D3*; see Karch et al. 1985), *abdA* protein appears in the epidermis and nervous system of the eighth abdominal segment and also in the rudimentary ninth abdominal segment, which appears on the dorsal surface of the embryo (Fig. 5B). Surprisingly, there is no apparent change in the *abdA* pattern in segments A1–A7, although *AbdB* protein is normally expressed in segments A5–A7 (Celniker et al. 1989). Two less extreme alleles are associated with rearrangement breaks that cut within the longer *AbdB* transcription units (.48 and .1065; see Celniker et al. 1989); these also give *abdA* staining in the eighth and ninth abdominal segments. Two *iab-8,9* rearrangements that break near the 5′ end of the longest *abdB* transcript (Uab^1 and *Tab*; see DeLorenzi et al. 1988) have no apparent effect on the *abdA* pattern.

iab *alleles* We examined the patterns of *abdA* protein expression in several classes of abdominal region mutations. Where possible, we examined deletions lacking the *AbdB* transcription unit, so that indirect effects through *AbdB trans*-regulation are not at issue, and mutant embryos could be identified by the transformed morphology of the posterior structures.

iab-7, iab-6 *Df(3)C4* removes the DNA of the complex from the *iab-7* region to the right, including the *AbdB* transcription unit (Fig. 5A). Embryos homozygous for this deficiency look like the extreme *AbdB* homozygotes (Fig. 5B). Embryos hemizygous for a synthetic deficiency extending distally from the $iab\text{-}6^{105}$ breakpoint look the same.

$T(Y;3)iab\text{-}7^{S10}$ is an insertional translocation of the left part of the complex into the Y chromosome (originally named $AbdB^{S10}$; Tiong et al. 1987); we mapped the break in the complex just to the left of the *AbdB* homeo box (Fig. 5A). We designated it as an *iab-7* because it does not break within the *AbdB*-coding region and because it re-

Figure 4. Doubly stained tissues. (*A–E*) The *Ubx* antigen was revealed by peroxidase staining (brown) and *abdA* was revealed by alkaline phosphatase (blue). (*A–C*) Embryos ~5, 8, and 12 hr old, respectively. (*D*) Dorsal view of a 10-hr embryo showing nuclei of the amnioserosa expressing *Ubx* or *abdA*. (*E*) The gut of a 12-hr embryo (the one in *C*). The anterior limit of expression of *abdA* in the visceral mesoderm meets the posterior limit of *Ubx* expression at the first major constriction of the midgut. The arrow points to a fragment of tracheal tissue adhering to the anterior midgut. (*F*) Rudimentary gut of an embryo ~9 hr old, taken from a line expressing β-galactosidase under control of the *ftz* promoter. The *ftz–lacZ* stripes are stained blue and are labeled by parasegment. The parasegmental identities were determined with reference to the segmented epidermis before the gut was dissected out. The *abdA*-expressing nuclei are stained brown. The staining in the visceral mesoderm cells begins in the PS8 *ftz* stripe. The arrow points to *abdA* expressing cells of the developing tracheal system, which adhere to the outside of the gut. (*G–I*) Nuclei expressing *abdA* are stained brown, and the surfaces of neuronal cells are stained blue (using anti-horseradish peroxidase). Pelts of late (~ 14 hr) embryos were photographed from the inside surface. (*G*) Lateral PNS of segments T3–A4. Anterior is at the top; dorsal toward the left. The scolopidia of the clustered chordotonal organs are marked with arrows. The nuclei in the epidermal groves at the A1/A2, A2/A3, and A3/A4 boundaries show *abdA* staining. Note the *abdA* staining in the chordotonal nuclei of A1, ahead of the anterior limit of epidermal staining. (*H*) The interior ventrolateral surface of segments A3 and A4. The ventral nerve cord is at the bottom. Arrows indicate the bipolar cells on the intersegmental nerves. The bipolar cell on the A2/A3 border is not stained, but the equivalent cells at the A3/A4 and A4/A5 boundaries have *abdA*. (*I*) The ventrolateral PNS of segments A4 and A5. The ventral nerve cord is at the *bottom*. The arrows indicate the paired *abdA*-expressing cells, which probably innervate the tracheal tubes. Bars, 50 μm (*A–F*); 20 μm (*G–I*).

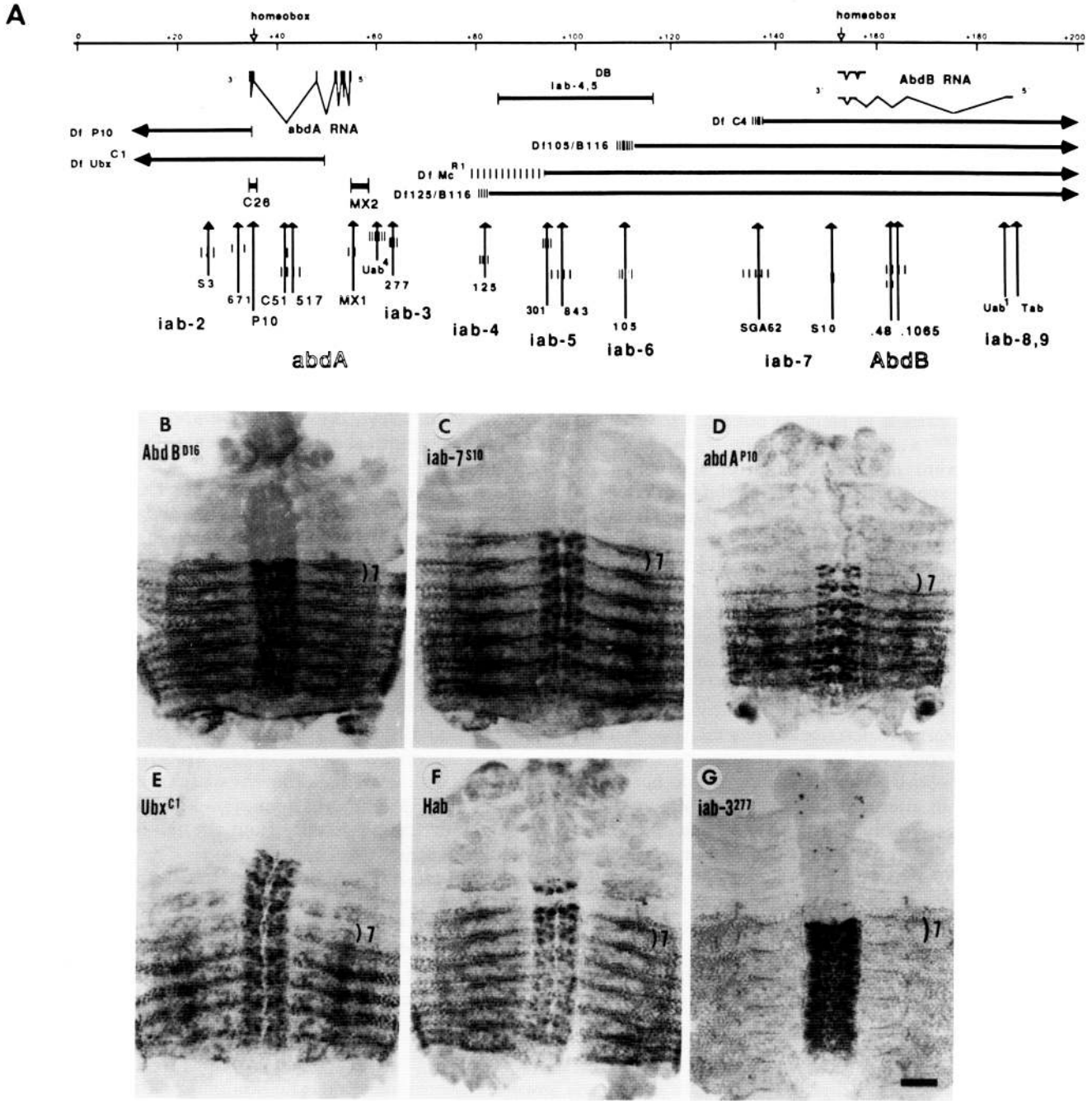

Figure 5. *abdA* pattern in mutants. (*A*) The thin line represents the genomic DNA of the abdominal region of the BX-C. Below the DNA line are the *abdA* and *AbdB* transcription units. The lesions are shown for mutations examined for *abdA* antigen; vertical arrows indicate rearrangement breakpoints, and horizontal bars indicate deletions. The position of *iab-7*^{S10} has not been reported previously. (*B–G*) Pelts of mutant embryos. The position of PS7 is marked on the epidermis of each embryo. (*B*) *AbdB*^{D16} homozygote. Note staining in the epidermis of the eighth abdominal segment and the small dorsal ninth abdominal segment. (*C*) *DpAbdB*^{S10}; *DfP9/DfP115*. Note staining in the epidermis of A8 but not in the ventral nerve cord. The nerve cord staining in A7 and A6 is also reduced. (*D*) *T(2;3)P10* homozygote. Note the loss of epidermal staining in the second abdominal segment (PS7). (*E*) *Ubx*^{C1} homozygote. The staining begins in the nerve cord and in the tracheal tubes of PS5. In PS6 and PS7, the pattern is unchanged, except that there is additional weak staining in cells underlying the lateral epidermis. In PS8–PS12, there is staining of the epidermal cells in the pattern of wild-type *abdA* (*F*) *Hab*/+. Cells in the nerve cord and epidermis of PS5 and anterior PS6 make *abdA* protein, and the staining intensity is enhanced in the anterior neural cells of PS7. This embryo is from a *Df(3)red/UbxP18* mother; *Hab* embryos from wild-type or *Hab* homozygous mothers also stain in PS5 and PS6, although typically in fewer cells. (*G*) *iab-3*^{277} homozygote. This embryo is older than the others shown, and the nerve cord has shortened relative to the epidermis. Several nuclei in the anterior nerve cord and brain lobes stain strongly for *abdA*. The anterior margin of the PS7 neural pattern is also enhanced. The photographs are all at the same magnification; the bar in *G* represents 50 μm.

sembles other *iab-7* alleles phenotypically. Embryos with *DpS10* on the Y chromosome and deficient for the BX-C on both third chromosomes (*DfP9/DfP115*) showed a posterior spread of *abdA* protein into A8 and A9, as expected for embryos lacking *AbdB* (Fig. 5C). However, there is a surprising loss of staining in the ventral nerve chord in A8, a strong reduction in A7, and a slight reduction in A6. This may be due to a Y chromosome position effect on *abdA*, but it is quite unusual in that it is restricted to the neural tissue and restricted to posterior segments. It does not seem typical of heterochromatic position effect in that the expression is not variegated, and the pattern is not changed when the embryos are raised at 18°C.

iab-5 Embryos with *iab-5* rearrangement breakpoints (*iab-5^{301}* or *iab-5^{843}*; see Fig. 5A), either homozygous or heterozygous with *iab4,5^{DB}*, could not be distinguished from wild type, even when dissected and examined at high magnification. In particular, there was no loss of staining in the somatic cells of the gonad or in the pericardial cells that underlie the epidermis of the fifth abdominal segment.

iab-4 The *Mc^{R1}* deficiency extends into the *iab-4* region (Fig. 5A; R. Hoppman and I. Duncan, pers. comm.). The pattern is similar to that of Figure 5B, but close examination shows that there is no staining of the intersegmental neurons (A4–A7), the gonad (A5), and the pericardial cells (A5–A7). Embryos hemizygous for a synthetic deficiency extending to the right from *iab-4^{125}* (Fig. 5A) have the same pattern as *Mc^{R1}* homozygotes. Homozygotes for the internal deficiency *iab4,5^{DB}* (Fig. 5A) also lack the additional staining of the intersegmental neurons, gonads, and pericardial cells of A4–A7.

iab-3 The available *iab-3* mutations are all associated with rearrangement breakpoints, and they cut the *iab-4* regulatory region away from the *abdA* promoter, as well as part of *iab-3*. In embryos homozygous for *iab-3^{277}*; the protein pattern in PS8–PS13 looks like a reiteration of the wild-type PS7 pattern (Fig. 5G). The embryos look like homozygous *iab4* embryos, except that the staining in A3–A7 looks less intense, because the intensity does not increase in the posterior segments as it does in wild type. There is apparently normal expression of *abdA* in the visceral mesoderm. The *iab-3^{277}* mutant embryos also show inappropriate expression in the thoracic and head segments (see below).

iab-2 *iab-2^{S3}* (formerly called *abdA^{S3}*) is a break at about +26 (Fig. 5A); it is among the weakest *iab-2* mutations, because it gives only a slight transformation of the adult second abdominal tergite to the first. We saw no change in the pattern of embryonic *abdA* expression. Embryos hemizygous for the *iab-2^{671}* breakpoint at +32 kb have lost most of the epidermal staining in PS7, although the pattern and intensity in the CNS appears normal (not shown). The breakpoint of *T(2;3)P10* is at +35, probably within the homeo box of the *abdA* transcription unit (Karch et al. 1985), and it is a lethal *abdA* allele. Embryos homozygous for *T(2;3)P10* or *DfP10* make antigen in a pattern like that of *iab-2^{671}* hemizygotes, except they show even less PS7 epidermal staining (Fig. 5D). The overall staining is also weaker, presumably because the truncated *abdA* mRNA or protein is unstable.

Misexpression mutants

Ubx^{C1} is an internal deletion in the complex removing the DNA between −51 and +50 kb (Rowe and Akam 1988). Rowe and Akam have shown that the *Ubx^{C1}* chromosome makes a hybrid RNA, with the 5′ exons of the *abdA* transcription unit joined to the 3′ exons of the *Ubx* transcription unit. Our sequence analysis predicts that the hybrid transcript would fuse protein-coding regions in-frame, joining amino acid 115 of *abdA* (end of exon 5) to amino acid 273 of *Ubx* (beginning of microexon 2). The hybrid protein should, and does, react with our antibody. *Ubx^{C1}* homozygotes show staining in PS5 in a pattern closely resembling the wild-type pattern of *Ubx* protein, although the staining in the epidermis is very weak relative to the nerve cord staining (Fig. 5E). PS6 and PS7 repeat the PS5 pattern, except that there is some additional staining in or under the lateral epidermis. The nerve cord pattern in PS5–PS7 is similar to the *Ubx* pattern of embryos deleted for all of the complex except for the *Ubx* transcription unit (W. Bender, unpubl.). There is no additional staining apparent in PS7, presumably because most or all of the *iab-2* regulatory region directing *abdA* in PS7 is deleted. Additional staining appears in the epidermis in PS8–PS12, just as these parasegments stain in *T(2;3)P10* (Fig. 5D), which deletes to +35. The *DfP10* embryos also show *abdA* staining in the ventral nerve cord in PS7–PS12, but in *Ubx^{C1}* there is no obvious addition to the staining pattern in the ventral nerve cord in PS7–PS12. We expect that the DNA between +35 and +50 specifies the pattern of *abdA* in the ventral nerve cord.

We examined several dominant mutations that are thought to misexpress *abdA*. The *Hab* mutation transforms the third thoracic segment toward the second abdominal (Lewis 1978). The penetrance is normally very weak, but for unknown reasons, the penetrance improves dramatically in offspring of *Hab* fathers and *Df(3)red/UbxP18* mothers. Among embryos of such a cross, we found some with abnormal staining in the third thoracic segment (Fig. 5F). The strongest staining cells appear in posterior T3, in both the epidermis and the ventral nerve chord, although some cells in anterior T3 and even in T2 stained more weakly. There is a striking absence of abnormally staining cells in anterior A1. Embryos from a *Hab* homozygous stock sometimes showed a few abnormally staining cells in posterior T3.

We also examined embryos of several mutations that produce an *Ultra-abdominal* phenotype, in which the adult first abdominal tergite is transformed to the second abdominal tergite, presumably due to misexpression of *abdA*. The *Uab^{1}* and *Uab^{5}* mutants have rearrangement breakpoints in the *bxd* regulatory region, and *Uab^{2}* breaks in the *Ubx* transcription unit. All three have near normal *abdA* expression patterns in embryos, with no apparent mis-expression in PS6. *Uab^{4}* is associated with a break in the *iab-3* region; *Uab4/+* em-

bryos have several cells in PS6 staining weakly for *abdA*, especially in the ventral nerve cord (not shown). Another *iab-3* allele, *iab-3*^{277}, shows a slight *Uab* phenotype when heterozygous with a deficiency (Karch et al. 1985). Embryos homozygous for the *iab-3*^{277} break show strong expression in a small number of cells scattered throughout the anterior nerve cord and brain lobes (Fig. 5G). The cells do not look random, because the pattern is largely bilaterally symmetric.

Discussion

Structure of the abdA *product*

The *abdA* gene resembles the *Antp* and *Ubx* genes in several respects. All are defined by lethal mutations whose lesions disrupt a large transcription unit. All three transcription units are transcribed in the same direction on the chromosome. All encode protein products with a homeo box. The three homeo boxes are quite similar; there are only four substitutions between *abdA* and *Ubx* (two are conservative) and five substitutions between *abdA* and *Antp* (three are conservative). There is another short peptide, YPWM, encoded within the fifth exon of *abdA* that is conserved in *Ubx*, *Antp*, *Dfd*, *Scr*, *lab*, and other vertebrate homeo box-containing genes (Mavilio et al. 1986; Krumlauf et al. 1987; Wilde and Akam 1987). As in *Ubx* and *Antp*, the *abdA* YPWM peptide is separated from the homeo box exon by a small microexon. Wilde and Akam (1987) reported a sequence Met-(Asn)-Ser-Tyr-Phe (MXSYF) lying at the amino terminus of the *Ubx* protein that is also found close to the amino terminus of the *Antp* and is the initiation sequence in the mouse gene *Hox-2.1* (Krumlauf et al. 1987). In *abdA*, we find a related sequence, Met-Asn-Ser-Tyr-Gln, starting at amino acid 37. The *abdA opa* $(CAA/CAG)_n$ encodes a stretch of polyglutamine downstream of the homeo box. Similar repeats are found in *AbdB*, *Ubx*, *Antp*, *Dfd*, *en*, *ftz*, and *lab*, where they encode strings of either glutamine, alanine, or serine. The functions of these homopolymer sequences are unknown. Aside from these features, the *abdA* protein is highly diverged from those of *Ubx* and *Antp*.

The *abdA* and *Ubx* products appear to have similar functions in the developing fly. The second abdominal segment (PS7) is similar to the first abdominal segment (PS6) in both larvae and adults. In some specific cell types, the *Ubx* and *abdA* products have identical effects. The *Ubx* product is needed to connect the dorsal tracheal trunks on the first-instar larva in PS5 and PS6, and *abdA* does the same in PS7–PS12 (Lewis 1978). Almost all cells of the PNS are morphologically unchanged between PS6 and PS7 despite the expression of *abdA* in many of these cells in PS7. The chordotonal cells are the conspicuous exception (see below).

The similarity of *abdA* and *Ubx* is also demonstrated by the functioning of the hybrid protein in the *Ubx*^{C1} mutation. This deletion apparently makes a fusion protein whose amino-terminal half is derived from *abdA* and whose carboxy-terminal half is derived from *Ubx*. The *Ubx*^{C1} hybrid protein can carry out wild-type function in PS5 and partially rescue the *abx/bx* mutations (Casanova et al. 1988; Rowe and Akam 1988). The fusion also gives some abdominal character to segments A3–A8, although *Ubx*^{C1} does not complement with *iab-3* alleles for the adult transformations of the sternites (F. Karch, unpubl.). Thus, the homeo box portion of the protein appears to be important, but not exclusive, for the character of the cellular transformations that the homeotic protein can specify.

The *abdA* protein does function differently from *Ubx* in some cell types. The five lateral chordotonal cells of the PNS express *abdA* from PS7 to PS12. Analogous groups of three chordotonal cells are found more dorsally in PS5 and PS6; these cells are expressing *Ubx* protein. In *abdA* mutants, the five abdominal chordotonal cells are transformed into the thoracic type group of three. Thus, the *abdA* product can direct the precursor cells of the chordotonal cells in a different pathway of development in PS7–PS12.

Building the pattern of expression of abdA

The pattern of *abdA* expression in embryos is much more uniform from segment to segment than are the patterns of *Ubx* or *Antp*. This might have been expected, because the second through seventh abdominal segments are morphologically quite similar in young larvae. However, there are discernible pattern differences in the different segments, and these are specified by the appropriate *iab* regulatory domains.

The buildup of *abdA* pattern is diagrammed in Figure 6, in the style used by Peifer et al. (1987). Embryos that are homozygous for a rearrangement break just 5′ to the *abdA* transcription unit (*iab-3*^{277}) have an intact *iab-2* regulatory region, but the *iab-3* and *iab-4* regions are cut away from the *abdA* promoter. These embryos show a normal pattern of *abdA* expression in PS7, and that pattern repeats without alteration in PS8–PS12 (Figs. 5G and 6A). The *iab-2* region can be subdivided into a region 3′ of the *abdA* homeo box, specifying epidermal expression, and a region within the introns of *abdA*, specifying expression in the ventral nerve cord. The *T(2,3)P10* breakpoint abolishes the PS7 epidermal expression (Fig. 5D), and the *Ubx*^{C1} deletion fails to turn on the PS7 pattern in either epidermis or nerve cord (Fig. 5E).

Embryos that have both the *iab-2* and *iab-3* regions intact (Fig. 6B) do not show any additional cells staining in embryos, although the epidermal staining in PS8–PS12 may be somewhat more intense (*DfMc*^{R1} or *Df125/B116*; embryos not shown). Embryos lacking the *iab-2* epidermal region [*T(2;3)P10* homozygotes; Fig. 5D] show weak PS8 epidermal expression that is near normal in pattern. Thus, we expect that the *iab-3* region specifies the same epidermal pattern as that of the *iab-2* region; the redundant information serves only to make the PS8 expression more intense. The *Ubx*^{C1} pattern (Fig. 5E) suggests that little or no neural expression is specified by the *iab-3* region.

Embryos with *iab-2–iab-4* intact show subtle additions to the pattern in PS9–PS12 (Fig. 6C). In particular,

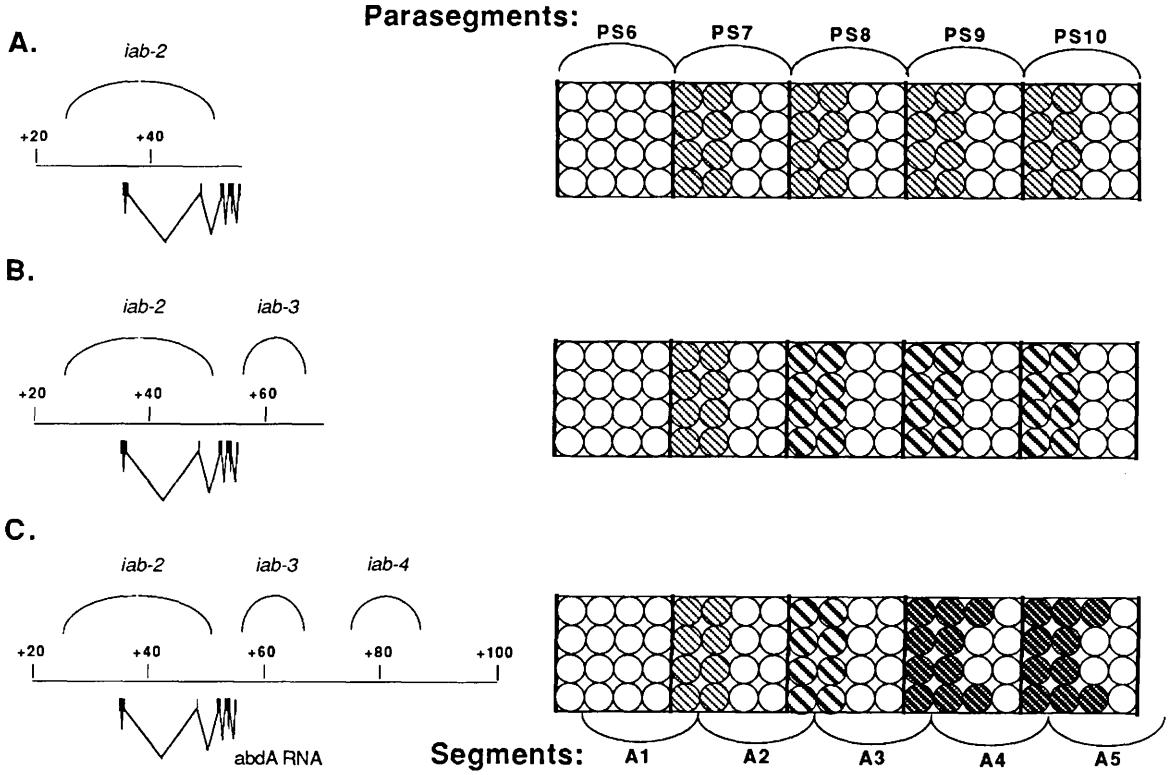

Figure 6. Buildup of the *abdA* pattern. The maps (*left*) indicate the extents of *abdA* regulatory regions in various genotypes. The diagrams (*right*) represent the cells of the embryonic ectoderm. The different types of shading indicate different levels of *abdA* protein. (*A*) Expression from *iab-2* alone. A pattern of expression appears in PS7, and the pattern repeats through PS8–PS12. (*B*) Expression from *iab-2* and *iab-3*. The pattern is unchanged except for slightly higher expression in the epidermal cells of PS8–PS12. (*C*) Expression from *iab-2*, *iab-3*, and *iab-4*. Epidermal protein levels are slightly enhanced, and additional cell types express in PS9–PS12.

the bipolar cell on the intersegmental nerve stains in PS9–PS12 (Fig. 4H). The *iab-4* region may also specify a subtle increase in the intensity of epidermal expression in PS9–PS12; there could be redundant pattern elements as in *iab-3*.

Embryos with an intact *iab-5* region, in addition to *iab-2–iab-4*, do not show any changes in the *abdA* pattern, specifically not in PS10–PS12. We had observed partial noncomplementation of nonoverlapping deficiencies in the abdominal region, based on adult phenotypes (Karch et al. 1985). Those results suggested that the *iab-5* region regulates both *abdA* and *AbdB* products. Our studies of *abdA* expression in embryos reported here do not support that suggestion, although regulation of *abdA* by the *iab-5* region might occur later in development.

The specification of the *abdA* pattern in mesodermal tissues is offset by one parasegment relative to the epidermis and nerve chord. Thus, expression in the visceral mesoderm, which begins in PS8, is specified by the *iab-2* region, not the *iab-3* region (it is apparent in *iab-3*^{277} homozygotes). Likewise, the gonad and pericardial cell staining, which occurs in the fifth abdominal segment (PS10), is specified by the *iab-4* region, not *iab-5*. There is a similar offset in the patterns of *Ubx* expression. Akam and Martinez-Arias (1985) noted that *Ubx* expression in the mesoderm of late embryos is shifted posterior one parasegment relative to the epidermal labeling. The *bxd* regulatory region directs *Ubx* expression in PS6 of the ectoderm and nervous system, but *bxd* mutations affect *Ubx* expression in the visceral mesoderm in PS7 (Bienz et al. 1988) and also transform the muscles of the body wall in PS7 (Hooper 1986). This shift in the expression domains in internal versus external tissues is difficult to understand, because the expression patterns of the gap and pair–rule genes, which presumably establish and number the segments, show no such shift.

In general, the pattern is built with positively acting regulatory elements; we have no indication of negatively acting regulation in the *iab-2*, *iab-3*, or *iab-4* regions. Busturia et al. (1989) argue for negative regulatory elements because they note slight posterior transformations, generally of the first abdominal segment, in some of the *iab-2*, *iab-3*, and *iab-4* mutations. However, these dominant gain-of-function transformations are each allele specific; adjacent breakpoints do not give similar posterior transformations. We interpret these transformations as position effects from the foreign DNA sequences that are juxtaposed to the *abdA* regulatory regions.

There is repression of *abdA* by *AbdB*, but only in the eighth and ninth abdominal segments. The boundary of

repression is at the posterior edge of A7, a segmental, not parasegmental, border. [It is not clear why *abdA* mutant embryos show subtle transformations in the cuticle of A8 (Morata et al. 1983; Tiong et al. 1985)]. *Ubx* expression is repressed by *abdA* in PS7–PS12 (Struhl and White 1985), and *Antp* is repressed by *Ubx* in PS5 and PS6 (Carroll et al. 1986). The *abdA* pattern is unchanged in *Ubx* mutants, and the *Ubx* pattern is not affected by *Antp* mutants. The general rule for these four homeotic genes is that each gene is repressed by the product expressed in the next posterior domain (Harding et al. 1985).

Gubb (1986) and Kornfeld et al. (1989) have proposed that the sizes of large transcription units may be timing the rapid events of early *Drosophila* development. Interestingly, there is a correlation between the size of the homeotic transcription units and the domain of expression in the embryo. The first *AbdB* mRNA detected belongs to the α, P3, or A class (Kuziora and McGinnis 1988; Celniker et al. 1989; Zavortink and Sakonju 1989), a 6.5-kb transcription unit. The 20-kb *abdA* transcription unit is shorter than the 75-kb *Ubx* transcription unit, which itself is shorter than the 103-kb *Antp* transcription unit. Perhaps *AbdB* would be the first homeotic product to appear, preventing overlapping expression of *abdA*. Likewise, *abdA* would have a head start in repressing *Ubx*, and *Ubx* would appear before the P1 products of *Antp*. However, we do not see any lag between the times of appearance of *abdA* and *Ubx* proteins, but we cannot rigorously compare the two without knowing the relative sensitivities of the two antibodies.

Evolutionary considerations

Mammals appear to have homologs to the *Drosophila* proteins of the Antennapedia and Bithorax Complexes, according to recent work on mice (Graham et al. 1989; Duboule and Dolle 1989). The homology in function seems clear, because the order along the chromosome of the fly and mouse homologs is maintained, and the mouse genes, like the fly genes, are expressed in order along the body plan in their chromosomal order. The similarity of the homeo box sequences of the segment-identity homeotics, especially among the *Antp*, *Ubx*, and *abdA* genes, suggests that all arose from a common ancestor, apparently before the divergence of vertebrates and arthropods. However, simple duplication mechanisms would not account for the invariant chromosomal order.

Akam et al. (1988) proposed a scheme for the origin of homeotic genes during evolution of the myriapod–insect lineage. They note that in *Drosophila* there is no direct correlation between the number of segments and the number of homeo box-containing genes. In their view, the *Ubx* and *abdA* genes, which belong to the *Antp* class of homeotics (and which may have no equivalents in vertebrates), appeared only in primitive insects and were absent from the myriapod-like ancestor that gave rise to insects. However, the finding of *Lox2*, identified as a *Ubx* or *abdA*-like homeotic gene, in leech (Wysocka-Diller et al. 1989) indicates that BX-C genes such as *Ubx* or *abdA* were indeed present earlier in evolution.

An alternative model is that the order came first, that an ancestral annelid had a tandem array of identical DNA units, one for each segmental unit of the body. The chromosomal regulatory units have evidently diverged far more in expression pattern than in the nature of the protein expressed, and two or more adjacent regulatory units may have evolved to direct a single homeo domain protein. Thus, the ancestral *abdA* gene may have been three genes, one for each parasegment, but now three regulatory regions direct a common transcript. Such a process of consolidation would reach limits. One could not differentiate PS7 from PS6 by expressing *Ubx* in additional cells, because *Ubx* is already expressed in nearly every nucleus of PS6. Thus, the extent of phenotypic differentiation from segment to segment constrains (and reflects) the number of distinct homeo box genes.

Materials and methods

Screening of the cDNA library and DNA sequencing

About 500,000 phages of an embryonic subpool of a cDNA library constructed by Michel Goldschmidt-Clermont were screened as described by Bender et al. (1983). We used as probe a *Bam*HI–*Sal*I fragment of 1.2 kb isolated from a phage that carries the 1.4-kb deletion of the $iab\text{-}2^{C26}$ deletion (Karch et al. 1985). This fragment contains the *abdA* homeo box but is deleted for the M or *opa* repeat lying at coordinates +35 kb on the DNA walk. Eight clones were selected, of which 1dB-5 carried the largest insert. Sequence analysis of the 1dB-5 cDNA was performed on both strands by the dideoxy nucleotide method of Sanger et al. (1977), using Klenow or Sequenase enzymes. Fragments resulting from four-cutter restriction enzyme digests were subcloned in the *Sma*I site of pEMBL8 or pEMBL9 vectors and grown as single-strand template (Dente et al. 1983) with the helper phage $M13^{K07}$. Genomic fragments that hybridized to the 1dB-5 cDNA were also subcloned in pEMBL and sequenced on one strand.

Production of abdA *fusion protein*

The whole 1dB-5 cDNA sequence, which was flanked by *Eco*RI sites, was introduced into the *Eco*RI site of the plasmid pEMBL8. The 1.1-kb *Pst*I fragment from position 613 (Fig. 2) to the *Pst*I site of the pEMBL8 polylinker (downstream of the *Eco*RI site at position 1767) was then inserted into the *Pst*I site of the bacterial expression vector pEX2 of Stanley and Luzio (1984). With the insert in the correct orientation, this plasmid has the potential to encode a protein composed of the pEX polypeptide (*Cro-LacZ*) fused at the carboxyl terminus to the complete *abdA* protein. The fusion includes 19 additional amino acids from the 613 *Pst*I site to the first ATG triplet at 669. To remove the polyglutamine stretch and part of the homeo box sequence from the fusion protein, we deleted the *Bgl*II fragment from position 1216 to 1733 (Fig. 2). Care was taken to perform all of the transformations and plasmid preparations at 30°C to avoid expression of the fusion protein. When the bacteria were grown above 30°C, spontaneous deletion events sometimes occurred. Analyses of the fusion protein were performed on cultures of 1.5 ml that were grown at 30°C to an OD_{550} of 0.2 and then shifted for 2 hr to 42°C to induce expression of the fusion

gene. Boiling the pellet of bacteria in sample buffer (Laemmli 1970) did not usually free the fusion protein; therefore, we first extracted them by standard boiling miniprep (I. Hope, pers. comm.). The soluble fraction was discarded, and the pellet (composed mostly of bacterial walls, chromosomal debris, and fusion protein) was sonicated in sample buffer for SDS–PAGE (Laemmli 1970). The lysate was run on 7.5% acrylamide gel, and the proteins were stained with Coomassie Brilliant Blue.

A fusion protein was also made to include most of the open reading frame upstream of the ATG at 669. A fragment extending from a *Bam*HI site in intron 3 to the *Pst*I site at position 613 in exon 4 was cloned into pEX2, as above. The fragment has a continuous open reading frame, in-frame with the protein-coding sequence shown in Figure 2.

To produce large amounts of fusion protein, a 200-ml culture was grown at 30°C to an OD_{550} of 0.2 and shifted to 42°C for 2 hr. Bacteria were collected by centrifugation and resuspended in 4 ml of 15% sucrose, 50 mM Tris, and 50 mM EDTA (pH 8.5). Then, 150 μl of lysozyme (10 mg/ml) was added, and the bacteria were left on ice for 15 min. Four milliliters of 0.1% Triton X-100, 50 mM Tris, 50 mM EDTA (pH 8.5) were added, and the lysate was centrifuged for 10 min in a 15-ml Corex tube at 12,000 rpm in a Sorvall HB4 rotor. The pellet was then resuspended in 4 ml of TE and sonicated until all viscosity disappeared. The homogeneous suspension was centrifuged again (10 min at 12,000 rpm) and resuspended in 4 ml of 2 M urea by sonication. This step was repeated with increasing amounts of urea to remove most of the insoluble proteins. Our fusion protein was only partly solubilized in 7 M urea. Usually, we stopped at 4 M urea, and the last pellet was resuspended and sonicated in 2 ml of water. The addition of 1 ml of 3× sample buffer (with SDS) clarified the white suspension, and the sample was boiled for 5 min with 5% β-mercaptoethanol and loaded onto two 7.5% SDS gels (wells were 3 mm thick and 120 mm wide). The proteins were revealed by immersing the gel in a cold solution of 0.1 M KCl. The fusion protein band was sliced out and washed for 1 hr in water to remove the KCl. After overnight electroelution at 50 volts in the presence of 50 mM NH_4HCO_3, 0.1% SDS (pH 8.0), the protein was precipitated with acetone, resuspended in 1 ml of water, and sonicated to obtain a white suspension. We estimated the yield of pure fusion protein at 2–5 mg.

Production and purification of antibodies

About 300 μl of protein (~1 mg) was mixed with 300 μl of complete Freund's adjuvant and injected at five spots behind the neck of a rabbit. Similar amounts in incomplete adjuvant were injected for the boosts. We obtained a useful serum after 2 boosts, although the rabbit was given 12 boosts over the course of 2 years. The serum was first depleted with an extract of pEX vector protein and then affinity-purified on a column coupled with *abdA*-pEX fusion protein. The extract of 200 ml of bacterial culture induced for the expression of the pEX protein alone was dialyzed against 0.1 mM MOPS, 0.1% SDS (pH 7.0), and coupled in the presence of 0.1% SDS to a 1 ml gel cake of Affigel-10-activated support (Bio-Rad), following the manufacturer's procedure. The affinity column was prepared by coupling the electroeluate of a 200-ml culture of *abdA*–pEX fusion protein to 0.3 ml of Affigel-10, also in the presence of 0.1% SDS.

About 5 ml of serum was depleted three times against the pEX column. Between each round, the antibodies reacting against the pEX protein were detached from the column with 3 volumes of 0.2 M glycine (pH 2.5). The depleted serum was then incubated overnight in a rotating tube at 4°C with the affinity column gel. The gel cake was then poured on a small column and washed with 15 ml of PBS, 0.1% BSA. The fraction bound to the affinity column was then eluted with 1 ml of 0.2 M glycine, 0.1% BSA (pH 2.5), and immediately dialyzed against phosphate-buffered saline at 4°C. Using this procedure, we obtained a serum with good affinity to *abdA* protein but with a relatively low titer.

The anti-*Ubx* antibody was the FP.3.38 mouse monoclonal of Rob White (a gift of Gary Struhl); the ascites fluid was used at a dilution of 1 : 1000. The anti-β-galactosidase was a mouse monoclonal from Promega; it was used at 1 : 1000. The anti-horseradish peroxidase was a rabbit polyclonal from Cappel (a gift of Michele Musacchio), also used at 1 : 1000.

Embryo staining procedure

Embryos were dechorionated, fixed, and devitellinized according to the procedure of Mitchison and Sedat (1983), modified by G. Struhl (pers. comm.). The fixed embryos were incubated with one or two primary antibodies diluted in BBT buffer [0.055 M NaCl, 0.04 M KCl, 0.015 M $MgSO_4$, 0.005 M $CaCl_2$, 0.02 M dextrose, 0.05 M sucrose, 0.1% BSA, 0.1% Triton X-100, 0.01 M Tricine (pH 7.0)] for ~12 hr at 4°C in a rotating tube. Embryos were then washed in BBT for 3 hr at 25°C in a rotating tube, with six changes of buffer. Embryos were incubated with secondary antibodies for at least 4 hr at 4°C. The secondary antibodies were goat-anti-mouse or goat-anti-rabbit coupled to horseradish peroxidase or alkaline phosphatase, all obtained from Bio-Rad and used at 1 : 1000 dilutions in BBT. The embryos were washed again in BBT for 3 hr at 25°C with six buffer changes. The embryos were washed briefly in 0.1 M ammonium citrate (pH 5.7) and soaked in the same buffer with 0.1% H_2O_2, 0.1% *p*-cresol, and 0.05% diaminobenzidine. The embryos were left in this staining solution for 5 min or until intense brown staining was apparent. To doubly stain embryos, the embryos were stained for alkaline phosphatase with the substrate kit III (blue) from Vector Laboratories, following the vendor's directions. The alkaline phosphatase staining was done either before or after the horseradish peroxidase staining, with equivalent results. Stained embryos were washed briefly with BBT and stored in BBT with 0.005 M azide at 4°C.

The embryo dissections were done with sharp tungsten needles and a dissecting scope with a 50-mm objective. The embryos were placed in a drop of Immu-mount (Shandon) for the dissection. Dissected pelts were transferred to a fresh drop of Immu-mount on a microscope slide and oriented at the edge of the drop, with the convex side up. The pelts were gently flattened under a coverslip, and the Immu-mount was allowed to solidify to make a permanent slide. For examination of cells internal to the epidermis, the pelts were mounted between two coverslips; the resulting sandwich could be examined from either side.

Lightly stained embryos were photographed with a Wratten no. 45 blue filter (Kodak) to enhance detection of the brown diaminobenzidine reaction product.

Strains and crosses

T(Y;3)iab-2^{671} was generated by Ed Lewis on a background chromosome carrying *In(3R)81/90C*; it is viable and fertile as a hemizygote, and it gives a partial transformation of the second tergite to the first. *T(2;3)abdA*^{517} is a complex rearrangement generated by Lewis; it is lethal when hemizygous and gives embryonic transformations like other strong *abdA* alleles. *In(3LR)iab-3*^{33} (breaks in 74A and 89E) was generated by Lewis on a background of *In(3R)81/92DE*; hemizygotes are viable but

sterile. *T(Y;3)B116* is a translocation with a break in 90E, also from Lewis. *Ubx^{C1}* was described by Rowe and Akam (1988). *iab-7^{S10}* (or *AbdB^{S10}*) was described by Tiong et al. (1987). *AbdB^{48}* was described by Celniker et al. (1989). The descriptions of the remaining mutations were reported in Karch et al. (1985).

The synthetic deficiencies beginning in *iab-4* and *iab-5* were generated by crossing females of *T(3;4)iab-4^{125}* or of *T(2;3)iab-5^{105}*, respectively, to males of *T(Y;3)B116*. The *iab/B116* sons were then crossed to *Df(3)P9/Dp(3)P5* females, and the resulting embryos were examined.

Embryos mutant or deficient for *AbdB* function could be recognized under the dissecting microscope from the altered morphology of the posterior spiracle rudiments. Embryos homozygous or hemizygous for *iab-4*, *iab-3*, or *abdA* mutations could be recognized under the compound microscope because they lack properly formed gonads.

Acknowledgments

We thank Nicole Wolff for excellent technical assistance. We are indebted to O. Acuto, C. Beall, N. Brown, and N. Richardson for their advice on handling insoluble proteins and immunopurification procedures, to G. Struhl for a gift of anti-*Ubx* monoclonal antibody, and to R. Bodmer for training in the anatomy of the PNS. We also thank Ed Lewis for sharing his unpublished *iab-2* and *iab-3* alleles. This work was supported by research grants from the state of Geneva and the Swiss National Fund (grant 3.365-0.86) to F.K. and from the National Institutes of Health (NIH) to W.B. and by a NIH postdoctoral fellowship to B.W.

The publication costs of this article were defrayed in part by payment of page charges. This article must therefore be hereby marked "advertisement" in accordance with 18 USC section 1734 solely to indicate this fact.

References

Akam, M.E. and A. Martinez-Arias. 1985. The distribution of *Ultrabithorax* transcripts in *Drosophila* embryos. *EMBO J.* **4:** 1689–1700.

Akam, M.E., I. Dawson, and G. Tear. 1988. Homeotic genes and the control of segment diversity. *Development* (suppl.) **104:** 123–133.

Beachy, P.A., S.L. Helfand, and D.S. Hogness. 1985. Segmental distribution of bithorax complex proteins during *Drosophila* development. *Nature* **313:** 545–551.

Bender, W., M. Akam, F. Karch, P.A. Beachy, M. Peifer, P. Spierer, E.B. Lewis, and D.S. Hogness. 1983. Molecular genetics of the bithorax complex in *Drosophila*. *Science* **221:** 23–29.

Bienz, M., G. Saari, G. Tremml, J. Müller, B. Züst, and P. Lawrence. 1988. Differential Regulation of *Ultrabithorax* in two germ layers of *Drosophila*. *Cell* **53:** 567–576.

Bodmer, R. and Y.N. Jan. 1987. Morphological differentiation of the embryonic peripheral neurons in *Drosophila*. *Roux Arch. Dev. Biol.* **196:** 69–77.

Breathnach, R. and P. Chambon. 1981. Organization and expression of eukaryotic split genes coding for protiens. *Annu. Rev. Biochem.* **50:** 349–383.

Busturia, A., J. Casanova, E. Sanchez-Herreo, R. Gonzales, and G. Morata. 1989. Genetic structure of the *abdA* gene of *Drosophila*. *Development* **107:** 575–583.

Carroll, S.B., R.A. Laymon, M.A. McCutcheon, P.D. Riley, and M.P. Scott. 1986. The localization and regulation of Antennapedia protein expression in *Drosophila* embryos. *Cell* **47:** 113–122.

Casanova, J., E. Sanchez-Herrero, A. Busturia, and G. Morata. 1987. Double and triple mutant combinations of the bithorax complex of *Drosophila*. *EMBO J.* **6:** 3103–3109.

Casanova, J., E. Sanchez-Herrero, and G. Morata. 1988. Developmental analysis of a hybrid gene composed of parts of the *Ubx* and *abdA* genes of *Drosophila*. *EMBO J.* **7:** 1097–1105.

Celniker, S.E. and E.B. Lewis. 1987. *Transabdominal*, a dominant mutant of the bithorax complex, produces a sexually dimorphic segmental transformation in *Drosophila*. *Genes Dev.* **1:** 111–123.

Celniker, S.E., D.J. Keelan, and E.B. Lewis. 1989. The molecular genetics of the bithorax complex of *Drosophila*: Characterization of the products of the *Abdominal-B* domain. *Genes Dev.* **3:** 1424–1435.

DeLorenzi, M., N. Ali, G. Saari, C. Henry, M. Wilcox, and M. Bienz. 1988. Evidence that the *Abdominal-B* r element function is conferred by a *trans*-regulatory homeoprotein. *EMBO J.* **7:** 3223–3231.

Dente, L., G. Cesareni, and R. Cortese. 1983. pEMBL: A new family of single stranded plasmids. *Nucleic Acids Res.* **11:** 1645–1655.

Duboule, D. and P. Dolle. 1989. The structural and functional organization of the murine HOX gene family resembles that of *Drosophila* homeotic genes. *EMBO J.* **8:** 1497–1505.

Duncan, I. 1987. The bithorax complex. *Annu. Rev. Genet.* **21:**285–319.

Gehring, W.J. 1987. Homeo boxes in the study of development. *Science* **236:** 1245–1252.

Graham, A., N. Papalopulu, and R. Krumlauf. 1989. The murine and *Drosophila* homeobox gene complexes have common features of organization and expression. *Cell* **57:** 367–378.

Gubb, D. 1986. Intron-delay and the precision of expression of homeotic gene products in *Drosophila*. *Dev. Gene.* **7:** 119–131.

Harding, K., C. Wedeen, W. McGinnis, and M. Levine. 1985. Spatially regulated expression of homeotic genes in *Drosophila*. *Science* **229:** 1236–1242.

Hiromi, Y., A. Kuroiwa, and W.J. Gehring. 1985. Control elements of the Drosophila segmentation gene fushi tarazu. *Cell* **43:** 603–613.

Hooper, J.E. 1986. Homeotic gene function in the muscles of *Drosophila* larvae. *EMBO J.* **5:** 2321–2329.

Karch, F., B. Weiffenbach, M. Peifer, W. Bender, I. Duncan, S. Celniker, M. Crosby, and E.B. Lewis. 1985. The abdominal region of the bithorax complex. *Cell* **43:** 81–96.

Kornfeld, K., R.B. Saint, P.A. Beachy, P.J. Harte, D.A. Peattie, and D.S. Hogness. 1989. Structure and expression of a family of *Ultrabithorax* mRNAs generated by alternative splicing and polyadenylation in Drosophila. *Genes. Dev.* **3:** 243–258.

Krumlauf, R., P.W.H. Holland, J.H. McVey, and B.L.M. Hogan. 1987. Developmental and spatial patterns of expression of the mouse homeobox gene, *Hox2.1*. *Development* **99:** 603–617.

Kuziora, M.A. and W. McGinnis. 1988. Different transcripts of the *Drosophila AbdB* gene correlate with distinct genetic sub-functions. *EMBO J.* **7:** 3233–3244.

Laemmli, U.K. 1970. Cleavage of structural proteins during the assembly of the head of the bacteriophage T4. *Nature* **227:** 680–685.

Laughon, A. and M.P. Scott. 1984. Sequence of a *Drosophila* segmentation gene: protein structure homology with DNA binding proteins. *Nature* **310:** 25–30.

Lewis, E.B. 1978. A gene complex controlling segmentation in *Drosophila*. *Nature* **276:** 565–570.

Martinez-Arias, A. and P. Lawrence. 1985. Parasegments and compartments in the *Drosophila* embryo. *Nature* **313:** 639–642.

Mavilio, F., A. Simeone, A. Giampaolo, A. Faiella, V. Zappavigna, D. Acampora, G. Poiana, G. Russo, C. Peschle, and E. Boncinelli. 1986. Differential and stage-related expression in embryonic tissues of a new human homeobox gene. *Nature* **324:** 664–668.

Mitchison, T.J. and J. Sedat. 1983. Localization of antigenic determinants in whole Drosophila embryos. *Dev. Biol.* **99:** 261–264.

Morata, G., J. Botas, S. Kerridge, and G. Struhl. 1983. Homeotic transformations of the abdominal segments of Drosophila caused by breaking or deleting a central portion of the bithorax complex. *J. Embryol. Exp. Morphol.* **78:** 319–341.

Mount, S.M. 1982. A catalog of splice junction sequences. *Nucleic Acids Res.* **10:** 459–472.

O'Connor, M.B., R. Binari, L.A. Perkins, and W. Bender. 1988. Alternative RNA products from the Ultrabithorax domain of the bithorax complex. *EMBO J.* **7:** 435–445.

Peifer, M., F. Karch, and W. Bender. 1987. The bithorax complex—Controlling segmental identiy. *Genes Dev.* **1:** 891–898.

Regulski, M., K. Harding, R. Kostriken, F. Karch, M. Levine, and W. McGinnis. 1985. Homeo box genes of the Antennapedia and bithorax complexes of Drosophila. *Cell* **43:** 71–80.

Rowe, A. and M. Akam. 1988. The structure and expression of a hybrid homeotic gene. *EMBO J.* **7:** 1107–1114.

Sanchez-Herrero, E., I. Vernos, R. Marco, and G. Morata. 1985. Genetic organization of the *Drosophila* bithorax complex. *Nature* **313:** 108–113.

Sanger, F., S. Nicklen, and A.R. Coulson. 1977. DNA sequencing with chain-terminating inhibitors. *Proc. Natl. Acad. Sci.* **74:** 5463–5469.

Stanley, K.K. and J.P. Luzio. 1984. Construction of a new family of high efficiency bacterial expression vectors: Identification of cDNA clones coding for human liver proteins. *EMBO J.* **3:** 1429–1436.

Struhl, G. and R.A.H. White. 1985. Regulation of the Ultrabithorax gene by other Bithorax Complex genes. *Cell* **43:** 507–519.

Tiong, S.Y.K., L.M. Bone, and J.R.S. Whittle. 1985. Recessive lethal mutations within the bithorax complex in *Drosophila*. *Mol. Gen. Genet.* **200:** 335–342.

Tiong, S.Y.K., J.R.S. Whittle, and M.C. Gribbin. 1987. Chromosomal continuity in the abdominal region of the bithorax complex of Drosophila is not essential for its contribution to metameric identity. *Development* **101:** 135–142.

Wharton, K.A., B. Yedvobnick, V.G. Finnerty, and S. Artavanis-Tsakonas. 1985. opa: A novel family of transcribed repeats shared by the Notch locus and other developmentally regulated loci in D. melanogaster. *Cell* **40:** 55–62.

White, R.A.H. and M.E. Akam. 1985. Contrabithorax mutations cause inappropriate expression of Ultrabiithorax products in Drosophila. *Nature* **318:** 567–569.

White, R.A.H. and M. Wilcox. 1984. Protein products of the bithorax complex in Drosophila. *Cell* **39:** 163–171.

———. 1985. Regulation of the distribution of Ultrabithorax proteins in Drosophila. *Nature* **318:**563–567

Wilde, C.D. and M. Akam. 1987. Conserved sequence elements in the 5′ region of the *Ultrabithorax* transcription unit. *EMBO J.* **6:** 1393–1401.

Wysocka-Diller, J.W., G.O. Aisemberg, M. Baugarten, M. Levine and E.R. Macagno. 1989. Characterization of a homologue of bithorax-complex genes in the leech *Hiduro medicinalis*. *Nature* **341:** 760–763.

Zavortink, M. and S. Sakonju. 1989. The morphogenetic and regulatory functions of the Drosophila *Abdominal-B* gene are encoded in overlapping RNAs transcribed from separate promoters. *Genes Dev.* **3:** 1969–1981.

Note added in proof

Sequence data described in this paper have been submitted to the EMBL/GenBank Data Libraries under accession number X54453.

abdA expression in Drosophila embryos.

F Karch, W Bender and B Weiffenbach

Genes Dev. 1990, **4:**
Access the most recent version at doi:10.1101/gad.4.9.1573